Journal of Power Sources, 42 (1993) 345–363

Premature capacity loss (PCL) of the positive lead/acid battery plate: a new concept to describe the phenomenon

D. Pavlov

Central Laboratory of Electrochemical Power Sources, Bulgarian Academy of Sciences, Sofia 1113 (Bulgaria)

(Received October 6, 1992; accepted November 5, 1992)

Abstract

When the lead–antimony grids in lead/acid batteries were substituted by lead–calcium ones, battery cycle life was dramatically shortened. This phenomenon was called first 'antimony-free effect' and later 'premature capacity loss' (PCL), 'early capacity decline' or 'relaxable insufficient mass utilization' (RIMU). PCL is encouraged by the following conditions: (i) lack of certain alloying additives as antimony, tin in the positive grid; (ii) high utilization coefficient of the positive active mass; (iii) low active mass density; (iv) no stack pressure on the positive plates in the cells, and (v) no capacity limiting role of H_2SO_4 in the cells.

Discharge of the positive active mass (PAM) proceeds through two successive reactions:

$$PbO_2 + 2H^+ + 2e^- \longrightarrow Pb(OH)_2\text{–'double-injection process'} \quad (1)$$

$$Pb(OH)_2 + H_2SO_4 \longrightarrow PbSO_4 + 2H_2O \quad (2)$$

For reaction (i) to proceed, equivalent amounts of H^+ ions from the bulk of the electrolyte and electrons from the plate grid should reach PAM. It has been established that PCL is due to the impeded transport of electrons when passing from the grid through the corrosion layer (CL) and PAM. A survey of the concepts of various authors for the reasons causing PCL has been made. PAM and CL have been treated as solid-state systems. Two general concepts have been distinguished. The first one assumes that PCL is due to the changes in PAM during cycling which result from the following phenomena: (i) impaired contact between PbO_2 crystals in the structure of PAM (Kugelhaufen model); (ii) changes in the intrinsic electrochemical activity of PAM (hydrogen-loss model), and (iii) changes in the α/β-PbO_2 ratio.

The second concept assumes that the changes in the electrical properties of the corrosion layer are the reason for the PCL effect. The latter is due to: (i) formation of a $PbSO_4$ barrier layer, and (ii) formation of a α-PbO semiconductor layer.

The present paper suggests a new approach to the structure of PAM which seems to unite all above concepts. PAM and CL are viewed as gel/crystal systems. Their particles and agglomerates are composed of α- and β-PbO_2 crystal zones which are in equilibrium with amorphous gel zones. The latter are built up of hydrated linear polymer chains along which electrons move between the crystal zones. Crystal zones have high electron conductivity. The electron conductivity of PAM is determined by the conductivity of the gel zones. To asses the effect of various conditions on this conductivity a tubular PbO_2 powder electrode was used. The surface of PAM particles are hydrated. Hence the electrode capacity will be determined by those particles whose hydrated surfaces are in electronic contact with one another and with the CL. The electrode capacity during the first and second cycles is a measure for the conductivity of gel zones at the CL/PAM interface. After 15 cycles

0378-7753/93/$6.00

the structure of the electrode is restored and its capacity depends on the conductivity of gel zones in PAM.

It has been established that the capacity of the tubular powder electrode depends on the density of PAM and on the additive to the grid alloy, to the solution and to PAM. A critical PAM density has been found to exist below which no restoration of the structure is possible. On plate cycling the volume of PAM pulsates, decreasing the density of PAM and of the CL. Gel zones play the role of 'hinges' in the skeleton of PAM making it elastic. When the active-mass density in a given region of PAM or in the outer CL sublayer falls below the critical value, this region is excluded from the current generation process and PCL may occur. It has been established that antimony lowers the critical value of the density and thus prolongs the life of the plate. Antimony ions get into the polymer chains improving the conductivity of the gel zones. The appearance of the PCL effect has been explained by the impact of dopants on the ratio gel/crystal zones and on the conductivity of gel zones in PAM and in the CL.

Introduction

When lead–antimony grids in lead/acid batteries are substituted by lead–calcium ones and the units are subjected to deep discharge cycling, battery life is dramatically shortened. This phenomenon is due to a decline in capacity of the positive plates, despite the fact that no visible damage to the positive-active mass (PAM) is observed and the plates are fully charged. The capacity loss precedes softening and shedding of the PAM. The phenomenon occurs in batteries that are produced with pure Pb, Pb–Ca, Pb–Ca–Sn and Pb–Sb (Sb < 1.5 wt.%) grids, in either pasted, tubular or Planté plates. Such behaviour was generally believed to be due to the lack of antimony in the grid alloy and, therefore, was termed the 'antimony-free effect'. Since early loss of capacity on cycling is also observed in batteries containing low-antimony alloys, the term 'antimony-free effect' has been replaced by 'premature capacity loss', PCL [1] or 'early capacity decline' (ECD). In this paper, the term PCL is adopted as a more accurate description of the general phenomenon.

Parameters influencing PCL

Based on the abundant data in the literature regarding the various battery types as well as the conditions of both preparation and cycling, the following basic parameters can be identified as exerting the strongest influence on PCL.

Alloying additives to grid alloys

Antimony

This element has the strongest effect on PCL. It has been established that battery cycle life decreases almost linearly with reducing the content of antimony in the grid alloy from 6 to 1% Sb [2]. An abrupt decline in performance is observed below 1 wt.% Sb.

Calcium

Figure 1(a) presents discharge curves for batteries with Pb–Ca grids. The battery life is very short [2]. This is due to the lack of antimony rather than to the presence of calcium, as can be demonstrated by covering the Pb–Ca grids with an antimony layer. Such batteries exhibit a capacity similar to that of Pb–Sb batteries until antimony (plated over the grids) is dissolved in the H_2SO_4 solution of the pores (Fig. 1(b)).

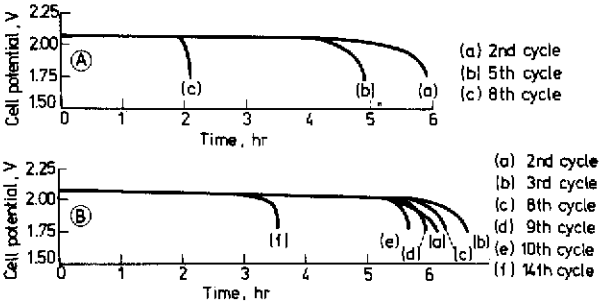

Fig. 1. Transient discharge curves for plates with: (A) Pb–0.09wt.%Ca grids, and (B) Pb–0.09wt.%Ca grids coated with antimony [2].

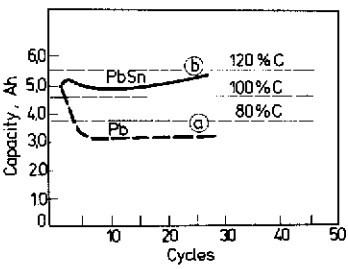

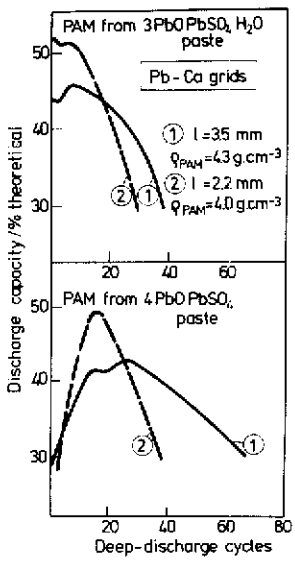

Fig. 2. Changes in capacity of 6 V/5 Ah batteries with: (a) pure Pb, (b) Pb–0.7wt.%Sn grid [3].

Fig. 3. Changes in capacity of positive battery plates prepared from $3PbO \cdot PbSO_4 \cdot H_2O$ and $4PbO \cdot PbSO_4$ pastes. (1) Plate thickness 3.5 mm, paste density 4.3 g cm^{-3}. (2) Plate thickness 2.2 mm, paste density 4.0 g cm^{-3} [4].

Tin

Nelson and Wisdom [3] have shown that tin in the positive grid alloy maintains a higher plate capacity on cycling as compared with that of plates with pure-lead grids (Fig. 2). Prolonged testing shows that the improved results are not always observed for Pb–Sn batteries. The addition of up to 1 wt.% tin to the alloys is insufficient to eliminate the PCL effect.

Active-mass density

Chang [4] has established that battery cycle life is enhanced by increasing the active-mass density and the plate thickness. Figure 3 presents the changes in capacity during cycling of plates with Pb–Ca grids produced from $3PbO \cdot PbSO_4 \cdot H_2O$ and

$4PbO \cdot PbSO_4$ pastes. The plates with greater thickness and higher density exhibit longer cycle life, but smaller capacity. When the active block is under stack pressure, the life of Pb–Ca batteries is improved substantially.

Amount and concentration of H_2SO_4

The life of positive battery plates with Pb–Ca–Sn grids that are affected by PCL phenomena is reduced when the H_2SO_4 concentration is increased. By contrast, decrease in the amount of H_2SO_4 in the cells causes batteries to exhibit longer cycle life [5]. With significant reduction of the quantity of H_2SO_4, the latter becomes a capacity-limiting active substance. When the amount of H_2SO_4 restricts the capacity to 60% versus that of batteries with excess of electrolyte, the cycle life of Pb–Ca–Sn batteries becomes commensurate with that of batteries that are unaffected by PCL. This performance has given rise to the starved-electrolyte design of battery.

Modes of charge and discharge

Nelson and Wisdom [3] have shown that PCL can be suppressed by conducting one, or several, deep discharges, as presented in Fig. 4. During the first discharge the capacity is low due to the onset of PCL phenomena. On the second discharge, that has followed a deep discharge, the plates exhibit their full capacity as a result of the processes that have taken place at the very low potentials of the first discharge cycle.

Hullmeine *et al.* [6] have found that Planté electrodes maintain a high and stable capacity when first charged up to 70% at the *C*/1 to *C*/2 rate and then charged at low current up to 15–20% overcharge. By contrast, if a charging rate of *C*/10 is applied up to an overcharge of 50%, the plates quickly lose capacity on cycling. This is illustrated in Fig. 5. No such effect of the charging mode has been observed with pasted battery plates.

Conditions favouring the PCL effect

PCL is encouraged by the following conditions: (i) lack of certain alloying additives, such as antimony, tin and others, in the positive grid alloy; (ii) high utilization coefficient of the positive active mass (η) and great depth-of-discharge (DOD), e.g., for automotive

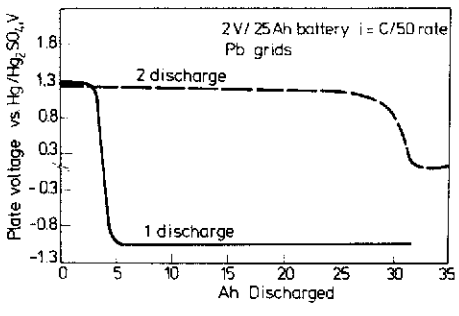

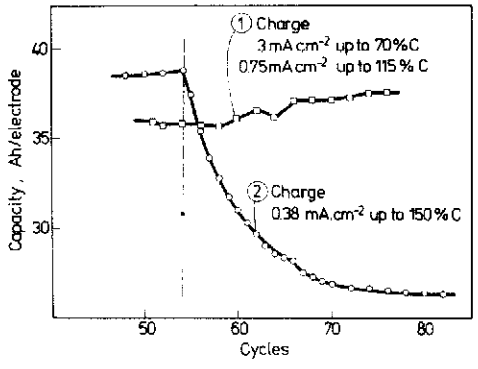

Fig. 4. Changes in potential of positive plate during discharge, 1st discharge: PCL is demonstrated, 2nd discharge: PCL phenomena are suppressed by phases obtained during first discharge down to −1.0 V with a current of *C*/50 [3].

Fig. 5. Effect of charge regime on capacity of Planté electrode [6].

batteries $\eta = 50$–55% and DOD = 50%, for traction batteries $\eta = 40\%$ and DOD = 80 or 100%; (iii) low-paste density; (iv) positive plates are not under stack pressure in the cells, and (v) no capacity-limiting role of H_2SO_4 in the cells. In order to determine which of the changes in the structural elements of the plates cause PCL, it is necessary to study the elementary processes that occur during discharge.

Mechanism of the processes of PAM discharge

Plate structure

As shown in Fig. 6, the positive plates of lead/acid batteries comprise: metal grid (Me), corrosion layer (CL) and lead dioxide (PbO_2) active mass (PAM). The corrosion layer is composed of two sublayers: (i) an inner, dense (compact) sublayer that covers the metal surface, and (ii) an outer, porous sublayer which is in contact with the active mass.

The PAM structure consists of the following two levels [7]:

(i) *Microstructure or agglomerate level.* The smallest building element is the PbO_2 particle. A large number of PbO_2 particles are interconnected into microporous agglomerates. It is at this level that the electrochemical process of battery discharge occurs.

(ii) *Macrostructure or skeleton.* Agglomerates are gathered together to form a macroporous skeleton. At this level, ion transport and formation of $PbSO_4$ crystals take place.

Elementary processes

During discharge, the reduction of the PAM proceeds in two stages [8]. In the first stage, the following electrochemical reaction takes place at the surface of the agglomerate micropores:

$$PbO_2 + 2H^+ + 2e^- \longrightarrow Pb(OH)_2 \quad (1)$$

The second stage commences when $Pb(OH)_2$ becomes in contact with the H_2SO_4 solution in the macropores:

$$Pb(OH)_2 + H_2SO_4 \longrightarrow (PbSO_4)_{sol} + 2H_2O \quad (2)$$

$$(PbSO_4)_{sol} \longrightarrow (PbSO_4)_{cr}$$

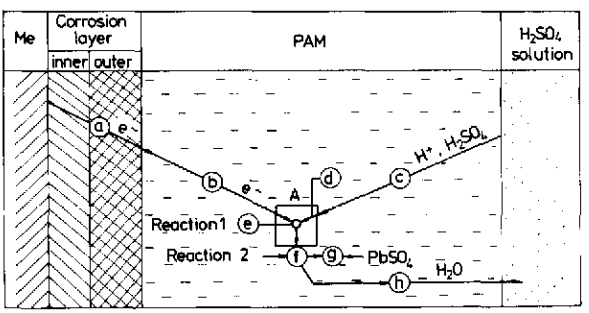

Fig. 6. Schematic representation of the elementary processes that occur on reduction of PbO_2 agglomerate A to $PbSO_4$ in skeleton of PAM.

Reactions (1) and (2) are separated in space, because of the limited access of H^+ and H_2SO_4 to the different structural levels of the PAM. H_2SO_4 cannot enter the micropores of the agglomerates because of their small radius and the relatively large size of the SO_4^- ions (the membrane effect).

Reaction (1) represents the so-called 'double-injection process'. This means that equivalent amounts of H^+ ions from the bulk of the electrolyte and electrons from the plate grid should reach the agglomerates for the reaction to proceed.

An agglomerate A, situated deep into the volume of PAM, will be reduced provided the following elementary processes occur (Fig. 6):

(a) electron transfer from the Mc through the CL to the PAM;

(b) electron transfer along the PAM skeleton to agglomerate A;

(c) transport of H^+ and H_2SO_4 from the bulk of the electrolyte along the macropores of PAM;

(d) transport of H^+ along the micropores of agglomerate A;

(e) occurrence of electrochemical reaction (1);

(f) occurrence of chemical reaction (2) and formation of $(PbSO_4)_{sol}$;

(g) nucleation and growth of $PbSO_4$ crystals in PAM macropores, and

(h) transport of water from agglomerate A along the macropores to the bulk of the solution.

Structural elements in which the phenomena leading to PCL occur

The plate capacity is limited by the elementary process occurring during current generation that proceeds at the lowest rate (statistically determined for the whole plate). When plate discharge proceeds with no PCL effects, the capacity-limiting elementary processes are associated with transport hindrances to the movement of H^+ and H_2SO_4 along the pores of the PAM (elementary processes (c) and (d)). The ion transport is impeded by the decreased pore cross section due to the formation of $PbSO_4$ crystals [9, 10]. These stages are reached when 50 to 60% of the PAM has been converted into $PbSO_4$ crystals (20-h discharge). PCL occurs much earlier, i.e., when 20 to 40% of the PAM has reacted. Therefore, the elementary processes (c), (d), (g) and (h) related to the transport of H^+, H_2SO_4 and H_2O, and the formation of $PbSO_4$ crystals are not responsible for PCL. Furthermore, it has been shown experimentally that the reduced cross section of the pores in PAM during discharge is not the cause of PCL [4].

Micropores have a fairly large surface area (3 to 7 $m^2\ g^{-1}$). The current density in the PAM is small. Hence, the electrochemical reaction (1) proceeds at low overcharge. It is also not responsible for the PCL.

The only possible reason remains the impeded transfer of electrons when passing from the grid through the CL and the skeleton of PAM to agglomerate A. Given this structural localization, the question arises: which phenomena create the PCL effect? An overview of suggestions put forward by various authors is presented in the next section of this paper.

PAM and corrosion layer: solid-state crystal systems that determine the PCL effect

PAM behaviour during battery cycling

Changes in the contacts between the PbO_2 crystals in the structure of PAM

According to Burbank and Ritchie [11, 12], when comprised of small prismatic PbO_2 crystals, the PAM is mechanically strong and elastic. As the PbO_2 crystals grow

in size, however, the contact between them is impaired and the plate capacity declines. PCL is due to the accelerated growth of PbO_2 crystals on cycling. This is observed in plates with either Pb–Ca or pure-lead grids. Antimony in the grid alloy increases the rate of PbO_2 nucleation and slows down crystal growth, and thus prevents the PCL effect.

Pavlov and Bashtavelova [7, 13] have established that, on plate cycling, the agglomerate structure of PAM obtained by metasomatic oxidation of the basic lead sulfate crystals disintegrate to fine PbO_2 crystals. The mechanical and electrical contact between these crystals is not reliable and the plate loses capacity. These phenomena are, however, more closely related to softening of the active mass.

The above-mentioned concepts assume that the size and morphology of PAM crystals and agglomerates determine the area and properties of the contact between them and, thus, the PCL effect. Winsel *et al.* [14] have adopted a reverse approach. They assume that the particles are spheres which implies that their type and morphology does not affect the PCL effect 'Kugelhaufen model'. Furthermore, these authors attribute some special properties to the contact between the spheres (neck zones) and claim that these properties determine PCL. The material in the neck zones is more thermodynamically stable and 'protected' during the reduction of PbO_2. PCL is due to an irregular growth of the electrical resistance in neck zones that is caused by a decrease in the cross-sectional area and to the formation of $PbSO_4$. This modifies the current distribution and large zones in the PAM are excluded from the electron-conductive network. As a consequence, the capacity declines. Either washing or thermal treatment of plates affected by PCL can restore the capacity as a result of solid-state relaxation of the neck zones. It has been suggested that the term PCL be replaced by 'relaxable insufficient mass utilization' (RIMU).

Changes in intrinsic electrochemical activity of PAM during cycling

Caulder *et al.* [15–18] have proposed a hydrogen-loss model. According to this concept, the electrochemical activity is determined by hydrogen that has been incorporated in the PbO_2 crystal lattice. It is argued that PAM contains two types of hydrogen: one that is bonded in water, and a 'free' one. The latter causes disorder of the crystal lattice. On cycling, the quantity of unbound hydrogen decreases. This leads to structural rearrangement of the disordered component of the PAM and, in turn, to a decreased electrochemical activity of PbO_2 and, hence, capacity loss.

Pohl *et al.* [19–22] have advanced the stoichiometry-changing current model. In this, hydrogen atoms ($H^+ + e^-$) are said to penetrate the PbO_2 crystal lattice and change the ratio Pb:O = 1:2 by a small amount, δ. Nonstoichiometric $PbO_{(2-\delta)}(H_2O)_\delta$ is obtained. The electrochemical activity of PbO_2 is determined by the number of sites occupied by hydrogen. Unbound hydrogen plays the role of a catalyst to the processes of deposition and reduction of PbO_2 [20]. Jorgensen *et al.* [23], and Hill *et al.* [24–27] have proved that hydrogen is present mainly as water adsorbed on the surface of PbO_2 crystals and in the form of hydroxyl ions [24–26]. They have established no correlation between PbO_2 electrochemical activity and hydrogen content [23, 24]. Furthermore, no relation has been found either between the structural disorder and the capacity of the plate [25, 27].

Maskalick [28] relates the electrochemical activity of PAM to the content of oxygen vacancies in the PbO_2 crystal lattice.

Influence of α and β modifications of PbO_2 on PCL

Dodson [29] has reported that the cycle life of positive battery plates is affected by the ratio between α-PbO_2 and β-PbO_2: the greater the amount of α-PbO_2 in the

PAM, the longer the life of the plate. Burbank [11] has established that though the content of α-PbO_2 decreases on cycling, the amount remaining in plates with Pb–Sb grids is higher than that in Pb–Ca counterparts. Caldera *et al.* [30] have reported that antimony has a strong effect on the amount of α-PbO_2 in the PAM and a much weaker influence on the content of the β modification. Hollenkamp [1] states that though the content of α-PbO_2 decreases on cycling it still remains in the skeleton of the PAM to form a 'backbone' that maintains the integrity of the PAM structure. Antimony facilitates the formation of α-PbO_2 and, thereby, strengthens the skeleton of PAM and prevents the PCL effect.

Changes in composition/properties of corrosion layer during cycling

The corrosion layer (CL) is composed of lead dioxide and nonstoichiometric lead oxide that can be reduced to $PbSO_4$ and/or PbO on discharge. If the content of these phases becomes significant, then the inherent high resistance may cause the CL to become a barrier to the passage of electric current.

Formation of $PbSO_4$ barrier corrosion layer

Tudor *et al.* [31] have established that on cycling batteries with Pb–Ca grids, the concentration of the $PbSO_4$ crystals near the grid increases and PCL is invoked. Weininger and Siwek [32] have reported that during float service of batteries, a high concentration of $PbSO_4$ is observed around the grid, but only at Pb–Ca grids and not in plates with Pb–Sn–Ca and Pb–Sb grids. Antimony and tin slow down the reduction of the corrosion layer. Rand *et al.* [33] have established that the amount of antimony is very small in regions of the CL with high $PbSO_4$ content. Hattori *et al.* [34] suggest that the $PbSO_4$ layer in the corrosion layer is interrupted. On cycling, the CL grows in thickness and forms two sublayers. On discharge, only the sublayer that faces the PAM is converted into $PbSO_4$. Nakashima and Hattori [5] assume that these $PbSO_4$ crystals form a semipermeable membrane [35–37] that stops the access of SO_4^{2-} ions to the corrosion layer and thus causes the neighbouring solution to become alkaline. This leads to the formation of α-PbO.

Formation of α-PbO barrier corrosion layer

Garche [38] suggests that on reduction of the PbO_2 in the CL, the presence of antimony promotes the formation of a fine $PbSO_4$ precipitate with membrane properties at the CL/pore-solution interface. The solution behind this membrane is alkalized and PbO is formed [35–37]. This sediment stops the further reduction of the CL and the electron transfer between PAM and the metal proceeds further only in the unaffected parts of the CL. Nakashima and Hattori [5] have reported that with Pb–Sn–Ca alloys, tin suppresses the formation of the PbO barrier layer. Giess [39] has also observed that tin decreases the rate of α-PbO formation. He has shown that when discharged positive plates are subjected to galvanostatic charging, the plates with Pb–Ca grids exhibit the highest polarization, while those with Pb–1.5 wt.%Sb grids display low polarization. The lowest corrosion-layer resistance has been observed in plates with Pb–Ca–0.6wt.%Sn grids. Hence, the PCL effect can be ascribed not only to a lack of antimony, but also to a deficiency of tin in the grid alloy (tin-free effect). Pavlov *et al.* [40] have explained the effect of tin in giving an increase in CL conductivity in terms of the semiconductive nature of PbO. On oxidation of the grid alloy, the resulting Sn^{3+} and Sn^{4+} ions occupy the sites in the PbO crystal lattice and give rise to a p-type conductivity. This allows the oxygen reaction to proceed and, in turn, allows the formation of nonstoichiometric $Pb(Sn)O_n$. The latter is a good conductor and hence

it reduces the polarization of the electrode during charge. Doring *et al.* [41] have applied this model and have assumed that the electric resistance appears mainly at the Pb/PbO_n interface, which is an n–p junction, and at the PbO_n/PbO_2 interface, p–n junction. In the presence of tin, the semiconductor junctions acquire an ohmic character.

Mechanical cracking of the corrosion layer

Douglas and Mao [42] have reported that when antimony-free plates are subjected to cycling and the corrosion layer grows in thickness, there appear mechanical stresses in it. The volume of PbO_2 is 20% greater than that of the lead from which it has been formed. The corrosion layer begins to crack and this impedes the contact between the PAM and the grid. This leads to PCL. In the presence of antimony, no such phenomena are observed. Mahato [43] has established that the number of cracks in the CL of pure-lead grids is much higher than that in Pb–Sb grids. Rand and collaborators [44] have found that the cracks in the CL on Pb–Sb grids tend to be located radially, while those in Pb–Ca grids generally are concentric. The latter have a stronger influence on the electric conductivity of the interface. Hattori *et al.* [45] have measured the hardness of the CL obtained on Pb–4wt.%Sb plate grids to be 54 kg mm^{-2}, and that on Pb–0.09wt.%Ca grids to be 88 kg mm^{-2}. Clearly, the antimony CL is more elastic and this makes it less susceptible to the formation of cracks.

Recapitulation of PCL concepts

In the above overview, the concepts advanced to date as explanations of the PCL effect were classified according to their structural features. The question remains: which of these concepts reflects best the real phenomena leading to PCL? It is very difficult to find the answer as there is no sound criterion for evaluation. Hence, each concept has its place in the battery theory. An alternative approach is also possible, namely, to look for a general phenomenon that will unite the above concepts. An effort in this direction will be made below.

PAM and corrosion layer: gel/crystal systems that determine the PCL effect

The gel/crystal structure of PAM

When the electron beam of a transmission electron microscope (TEM) is passed through the agglomerates and particles of PAM, an image of the type presented in Fig. 7 is obtained. In this, particles and agglomerates are characterized by a non-homogeneous mass distribution. The dark zones are the α-PbO_2 or β-PbO_2 crystal structure, while the lighter regions indicate amorphous and hydrated zones [46–49]. Hydrated zones occupy about 30% of the PAM [47]. The hydrated and crystal zones are in equilibrium [48]. Hydrated zones are also in equilibrium with ions in the solution, and this makes the PAM an open system. As a result of these experimental findings, a new concept for the structure of PAM particles and agglomerates has been suggested. It views the PAM as a gel system, the major part of which has crystallized to form α-PbO_2 or β-PbO_2 zones [49]. Gel zones are built of hydrated, linear, polymer chains of the type:

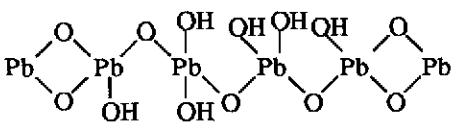

(a)

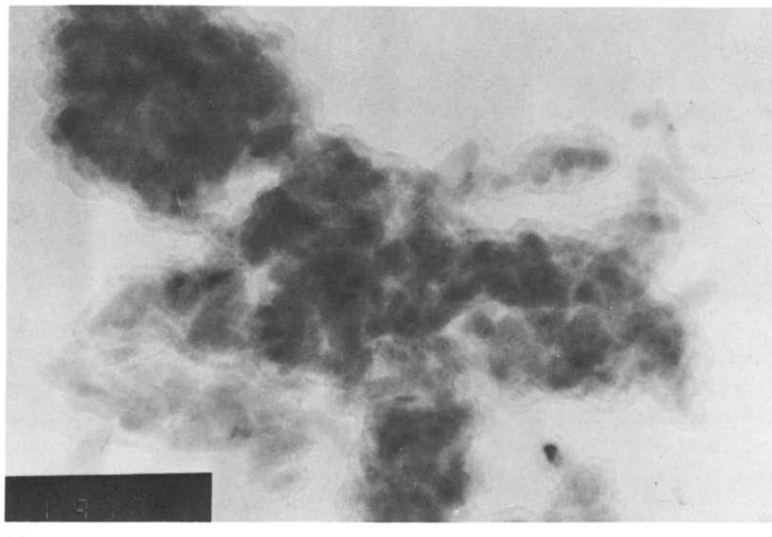

(b)

Fig. 7. TEM micrographs of PAM particles.

These chains have both electron and proton conductivity, which is a necessary condition for reaction (1) to proceed. Electrons move along the polymer chains overcoming low potential barriers. Hence, PAM agglomerates and particles acquire a microstructure of the type presented in Fig. 8 [49]. The crystal zones are 'islands' in which electrons move freely (n-type degenerated semiconductor). The gel zones contain polymer chains that play the role of 'bridges' along which electrons move between the 'islands'.

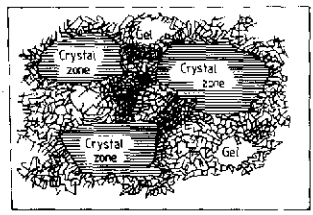

Fig. 8. Schematic view of parts of microstructure of PAM particles or agglomerates [49].

The gel/crystal structure influences the plate capacity: when the PAM is built only of PbO_2 crystals, it will have a high electron conductivity, but its proton conductivity will be low. The capacity of the plate will be low. Such is the case with PbO_2 that is prepared via chemical methods. By contrast, if the PAM is composed only of gel, it will exhibit a high proton conductivity, but a low electron conductivity. The plate capacity will be low again. If PAM is a gel/crystal system, both its electron and proton conductivities will be high and, equally, the plate capacity will be high. Hence, the dependence of plate capacity on PAM crystallinity passes through a maximum.

Up to now, investigations of PCL phenomena have been conducted according to the classical scheme, i.e., the capacity decline on cycling has been studied. We have adopted the reverse scheme [50]. In this procedure, the PAM was disintegrated into powder (agglomerates). Tubular electrodes, with central spines, were filled with the PAM powder. These electrodes were then subjected to cycling with the aim of determining those parameters that affect the rebuilding of the electrode structure. Building and disintegration of the electrode structure involve the same processes in the same structural elements, but proceed in opposite directions.

The surfaces of PAM agglomerates and particles are known to be hydrated. A given agglomerate will take part in the formation of the capacity if the polymer chains of its gel zones are connected with those of the adjacent agglomerates and these, in turn, are in contact with the corrosion layer. In this case, the capacity of the tubular powder electrode can be an indirect indication of the electron conductivity of the gel zones.

Dependence of electrode capacity on PAM density

Figure 9 presents the specific capacity, τ (Ah g^{-1}), of tubular powder electrodes with various PAM densities as a function of cycle life [50]. There is a critical value of the powder density (viz., 3.40 g cm^{-2}) above which restoration of PAM structure commences. Below this density, the number of polymer chains that connect the crystal zones of adjacent agglomerates is small and many agglomerates are excluded from the electrochemical process. On increasing the density of PAM, the gel at the contact zones between the agglomerates is concentrated. Consequently, the number of parallel polymer chains that connect the crystal zones is increased and, therefore, so is the electrode capacity.

How can a change in PAM density cause PCL? Figure 10 presents the values for the plate thickness as measured on charge and discharge at the 5th and 30th cycles [7]. During cycling, the plate pulsates. The volume of PAM grows on discharge due to the formation of $PbSO_4$ crystals, and shrinks when these crystals are oxidized to PbO_2. Because this is not always a reversible process, the PAM volume grows and the apparent density decreases [7]. The following conclusions can be drawn from this phenomenon:

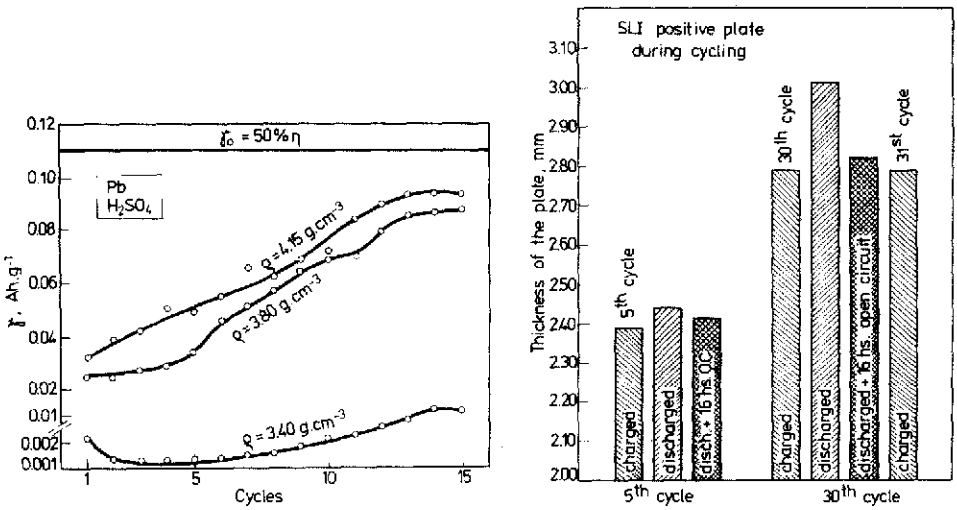

Fig. 9. Specific capacity of tubular electrodes as function of cycle number; effect of PAM powder density [50].

Fig. 10. Changes in thickness of an automotive (SLI) positive plate at 5th and 30th cycles; charged, discharged and kept at open-circuit for 16 h after discharge.

(i) If the PAM was merely a solid-state crystal system, pulsation would cause many of the solid-state necks between the agglomerates to be cracked or broken. By contrast, in gel/crystal systems, the gel zones take over and restrain the inner stresses and thus play the role of hinges in the skeleton of the PAM.

(ii) As a result of PAM pulsation, the apparent density in certain zones of the plate may decrease and reaches values below the critical limit and thus causes the electrode capacity to decline and the PCL effect to appear.

It follows then that one of the prerequisites for premature capacity loss is PAM pulsation on cycling. Valeriote *et al.* [51] have found that when the plates of the active block of the lead/acid cell are stacked (as a sandwich), no PCL is observed – even with Pb–Ca grids. This sandwich design can, however, cause ion-transport hindrances. The elementary processes (c) and (d), Fig. 6, may become capacity-limiting factors and thus cause the plate to lose part of its capacity.

Influence of dopants (additives) on PCL

To date, it is established that antimony is the dopant that exerts the strongest influence on PCL.

Effect of dopants when added to the solution

Figure 11 illustrates the changes in capacity on cycling tubular powder electrodes with powder densities 3.80 and 4.15 g cm^{-3}, and pure-lead spines. Antimony ions were added to the solution at the 6th and 12th cycles [50]. When the PAM density is close to the critical value, antimony ions hamper the process of building of the PAM structure. The higher the concentration of antimony ions, the stronger their effect. At a PAM density of 4.15 g cm^{-3}, the effect of antimony ions is significantly suppressed.

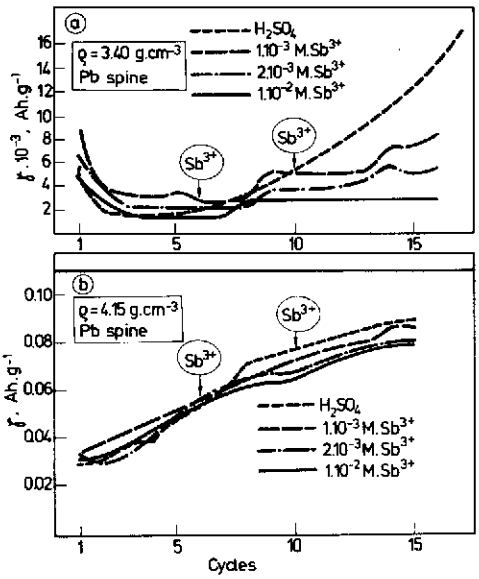

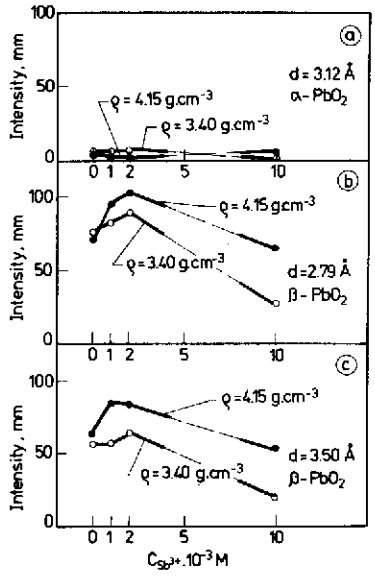

Fig. 11. Effect of antimony ions in H_2SO_4 solution on specific capacity of tubular powder electrodes [50].

Fig. 12. Dependence of intensity of characteristic diffraction lines for α-PbO_2 (d=3.12 Å) and β-PbO_2 (d=3.50 Å and 2.79 Å) on concentration of antimony ions in solution and on density of PAM [50].

Figure 12 presents the changes in intensity of the characteristic X-ray diffraction lines for α-PbO_2 and β-PbO_2 in cycled PAM as a function of the concentration of antimony ions in the solution [50]. An increase in the density of the PAM leads to higher crystallinity. The reason for this is the greater amount of substance in a unit volume (i.e., a smaller pore volume). It can also be supposed, however, that the density of PAM affects the equilibrium crystal/amorphous zones. Since agglomerates are an open system, an increase in the PAM density will cause the gel zones to undergo dehydration and their density to grow. Concomitantly, the number of parallel polymer chains that connect the crystal zones grows, and so does the electrode capacity.

Figure 13 presents the capacity curves for powder electrodes with lead and Pb–6 wt.%Sb spines when arsenic, bismuth or antimony ions are added to the solution [52]. Arsenic ions block the building of the PAM structure. By contrast, bismuth ions accelerate the process(es). The presence of antimony in the spine alloy causes the capacity to grow, even during the first cycle. This indicates that the CL and the CL/PAM interface each exert their own effect on the electrode capacity, i.e., on PCL.

Effect of dopants introduced into the alloy

Figure 14 shows the dependence of the specific capacity of tubular powder electrodes at the 1st, 5th, 10th and 15th cycles on the antimony content of the spine alloy [50]. The following conclusions about the impact of antimony in the alloy both on the CL/PAM interface and on PAM itself can be drawn from the data presented.

CL and CL/PAM interface. During the first cycles, antimony oxidized from the grid alloy is located in both the CL and the PAM particles that are in contact with

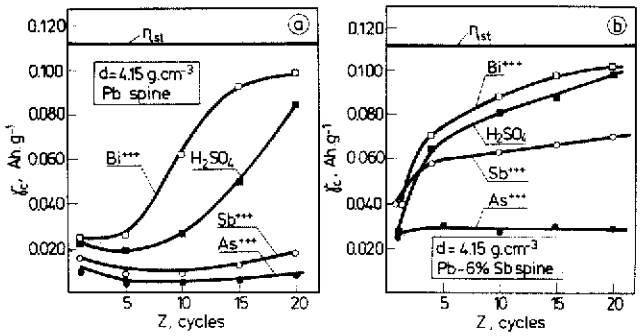

Fig. 13. Influence of arsenic, bismuth and antimony ions in solution on specific capacity during cycling of tubular powder electrodes with: (a) pure Pb, and (b) Pb–6wt.%Sb spines [52].

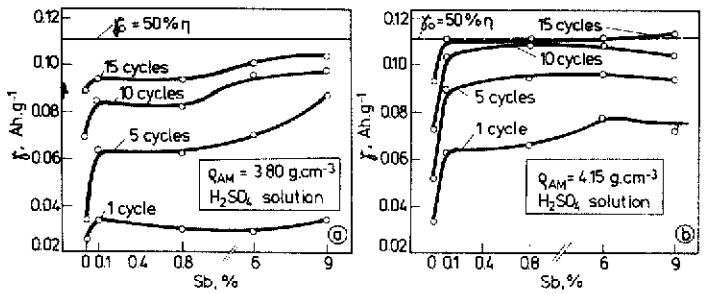

Fig. 14. Effect of antimony content in spine alloy on specific capacity of tubular powder electrodes at 1st, 5th, 10th and 15th cycles [50].

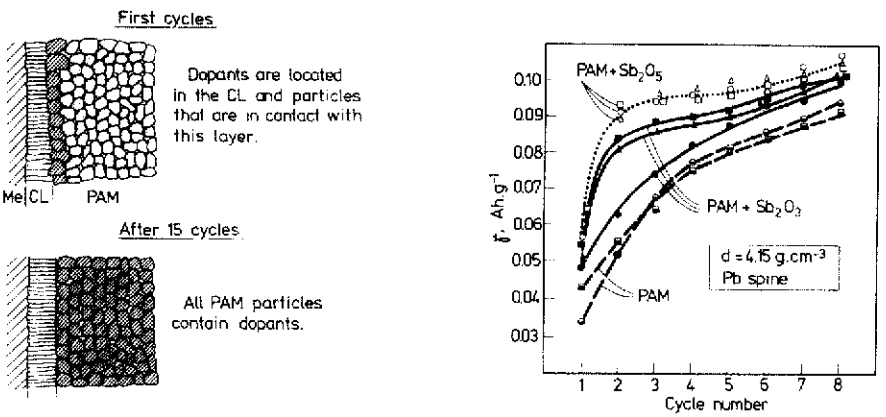

Fig. 15. Schematic representation of the electrode during 1st and 15th cycles. For 1st cycle, gel zones in hatched particles of PAM have absorbed antimony ions. The effect of antimony on the CL/PAM interface is evaluated from the capacity. At 15th cycle, antimony has been absorbed by the whole PAM. The effect of antimony on PAM is assessed from the capacity.

Fig. 16. Changes in specific capacity on cycling of tubular powder electrodes prepared with PAM doped with Sb_2O_3 or Sb_2O_5, or with no additives.

this layer (Fig. 15(a)). The capacity difference $\Delta\gamma = \gamma_{(Pb-Sb)} - \gamma_{Pb}$ shows that when 0.1 wt.% of Sb is added to the alloy, the specific capacity grows by 85% during the first cycle for electrodes with a powder density of 4.15 g cm^{-3}, and by 33% for electrodes with a density of 3.80 g cm^{-3}. This fact suggests that antimony ions affect the gel zones at the CL/PAM interface. The ions probably increase the number of polymer electric chains that connect the crystal zones in the corrosion layer with those in the PAM particles.

The electric conductivity of the CL/PAM interface depends on the ratio of gel/crystal zones in the CL and in PAM. Gel zones in the PAM amount to about 30% [47], while their content in the CL is 10% for pure-lead electrodes and 15 to 18% for Pb–Sb ones [53]. It can be expected that the high crystallinity of the CL formed on lead spines will render this interface rather sensitive to both mechanical stresses and thermal effects. There is probably a certain critical value of the ratio of gel/crystal zones above which mechanical stresses are suppressed and the interface does not crack. By introducing antimony to the alloy, the quantity of gel zones is significantly increased and this critical value is exceeded. Hence, a search should be made for alloying additives that will increase the quantity of gel zones in the CL.

Pavlov *et al.* [54] have shown that on oxidation of Pb–Sb electrodes, doped $Pb_{(1-x)}(Sb)_yO_n$ and $Pb_{(1-x)}(Sb)_yO_2$ oxides are formed. Antimony is also incorporated in the crystal lattice. These oxides have a higher electric conductivity than their pure-lead analogues. During cathodic polarization, $Pb_{(1-x)}(Sb)_yO_2$ is reduced at a potential that is 0.2 V more negative than that for nondoped PbO_2. This allows the reduction of the corrosion layer to start after the major part of the PAM has already been consumed.

PAM. The effect of antimony on the PAM can be evaluated by the specific capacity at the 15th cycle, see Fig. 15(b). Figure 14 shows that electrodes with a density of 4.15 g cm^{-3} ensure 50% PAM utilization even if only 0.1 wt.% Sb is added to the alloy. At a PAM density of 3.80 g cm^{-3}, the presence of antimony increases the active-mass utilization by 2 and 8% for electrodes containing 0.1 and 9 wt.% Sb in the alloy, respectively. Therefore, antimony makes the gel zones less sensitive to a decrease in PAM density by increasing their conductivity. Nevertheless, not all types of antimony ions exhibit this effect.

Effect of dopants when added to PAM

Sb_2O_3 or Sb_2O_5 were added to PAM powder contained in tubular electrodes. The capacity curves for the electrodes are presented in Fig. 16 [50]. It can be seen that Sb_2O_3 and Sb_2O_5 increase the specific capacity during the first cycle. Their effect is analogous to that of antimony when added as an alloying additive and opposite to the effect of antimony ions added to the solution. It is not certain, however, whether Sb_2O_3 does not undergo oxidation and whether its effect is not due to the pentavalent antimony that would thus be obtained.

Dawson *et al.* [55, 56] have established that when added to 4.5 M H_2SO_4 solution, antimony forms the complex ion $SbO \cdot SO_4^-$, and that $(Sb_3O_9)^{3-}$ is produced on the corrosion of Pb–Sb battery grids. When $SbO \cdot SO_4^-$ ions get into the gel zones, they may cause the polymer chains to separate from each another and thus slow down the transfer of electrons between them. This will decrease the electron conductivity of the gel zones. By contrast, when $(Sb_3O_9)^{3-}$ ions enter the gel zones, the electron conductivity of the latter grows and, hence, the electrode capacity increases. The type of dopant ions used influence the capacity and the PCL effect accordingly.

Difference between PCL and passivation of the positive plate

As with PCL, passivation of the positive plate (PPP) leads to a decline in capacity. Nevertheless, the phenomena responsible for these two effects are different. PCL is associated with changes in plate capacity but the chemical composition of the corrosion layer remains unchanged. During charge and discharge, the ratio $PbSO_4/PbO_2$, PbO_n are changed but not the nature of the $Me/CL_s/PAM$ chain (system). The specific resistance of the latter remains constant.

According to Lander [57] and Garche [38], under certain conditions some solid-state reactions proceed between Me and PbO_n, PbO_2 that cause the valency of the oxide in the corrosion layer to be reduced to $PbO_{n-\delta}$ or PbO. The resistance of the chain $Me/CL_s/PAM$ grows, in accordance with the stoichiometric coefficient of the oxide. These processes cause PPP.

According to Bullock and Butler [58], PPP is associated with the formation of an uninterrupted PbO sublayer in the corrosion layer, which has a high electric resistance and forms the electrode system: $Pb/PbO/PbO_2/H_2SO_4$.

Figure 17 presents the discharge curves of passivated positive plates. The discharge transient can feature one or two potential plateaus. Figure 17(b) shows that the first plateau reflects a potential arrest at low electrode polarization, and the second an arrest at considerably more negative potentials. The sum of the durations of the two steps is fairly close to that of the discharge of nonpassivated plates. As the major part of the discharge is carried out at potentials below the cutoff potential, the capacity of the electrode is low.

Passivation of the positive plate occurs when:

- the formed plates are dried for long periods at temperatures higher than 100 °C (thermopassivation) [59]
- the battery is kept in store for a long time (storage passivation) [60]
- a battery with antimony-free grids is left to operate in a floating mode without discharge at a voltage of about 2.24 V (floating passivation) [58, 61]
- a battery is discharged with a very weak current [62]

Takahashi *et al.* [62] describe the difference between PCL and PPP as follows:

(i) PCL is related to phenomena occurring in the outer corrosion sublayer, i.e., at the CL/PAM interface. These phenomena can be suppressed by introducing tin into the grid alloy and by reducing the amount and the concentration of H_2SO_4 in the solution.

(ii) Passivation (PPP) of the positive plate proceeds in the inner corrosion sublayer at the CL/metal interface. By contrast to PCL, decrease in H_2SO_4 concentration encourages PPP. Takahashi *et al.* [62] have found that passivation of the positive plate occurs in batteries with Pb–Sn–Ca grids and $H_2SO_4/PbO_2 < 0.6$.

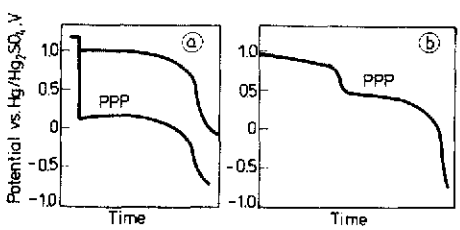

Fig. 17. Two types of potential change of passivated positive plates (PPP) with time of discharge.

To date, the following methods have been suggested for the prevention of positive plate passivation:

(i) Introduction of alloying additives (e.g., tin, antimony, etc.): these additives play the role of dopants and improve the p-type conductivity of the oxide and thus reduce the resistance of the corrosion layer [40]. Dopants can be introduced either directly to the grid alloy or in the form of a metal coating over the grid [60, 62].

(ii) Destruction of the passive layer by polarizing the plate to potentials equal to -1 V versus Hg/Hg_2SO_4, see Fig. 4 [3]. The changes in the phase composition of the CL result in an increase in its conductivity.

(iii) Continuous and intense evolution of oxygen [58]: the latter penetrates the PbO layer and oxidizes it to nonstoichiometric PbO_n with high electric conductivity. The intense oxygen evolution may, however, cause a PCL effect. This is because oxygen is released at the interfaces of the crystal/amorphous zones in the volume of the agglomerates. It may break down the polymer chains in the gel and decrease the conductivity at the contacts between the agglomerates in PAM as well as at the PAM/CL interface.

Comparison of gel/crystal concept with other proposed concepts

The gel/crystal structure and its properties provide an adequate basis for interpretating the physical nature of the phenomena that lead to PCL. In particular, it can account for the following theories that have been advanced by other research groups:

(i) The role of the contact between the crystals, agglomerates and 'spheres' in PAM as discussed in the papers of Burbank and Ritchie, Winsel and Voss, and Pavlov and Bashtavelova is related to the electrical properties and concentration of the gel zones that connect the particles, agglomerates and parts of the PAM skeleton and the PAM/CL interface.

(ii) The hydrogen models for the electrochemical activity of PbO_2 developed and investigated by Caulder and Simon, Pohl and Rickert, and Hill *et al.* can be associated with the effect of the proton conductivity of gel zones on the mechanism of the discharge process.

(iii) The influence of α-PbO_2 and β-PbO_2 on the integrity of the PAM structure reported by Dodson, Burbank, Rand and Hollenkamp can be explained by the different effects of these modifications on the equilibrium between the crystal and gel zones, and hence on the capacity of the system.

(iv) The effect of the mechanical strength and electrical conductivity of the PAM/CL interface disclosed in the studies of Rand, Hattori, Nelson, Takahashi and their collaborators can be related to the ratio between the gel and crystal zones and to its effect on the elasticity of the CL/PAM interface and on its conductivity.

Therefore, the above four concepts can be regarded as different manifestations of one and the same phenomenon that leads to PCL. The suggested gel/crystal structure approach is a synthesis of all these concepts in an integral theory.

References

1 A. F. Hollenkamp, *J. Power Sources, 36* (1991) 567–585.

2 K. Fuchida, K. Oxada, S. Hattori, M. Kono, M. Yamane, T. Takayama, J. Yamashita and J. Nakayama, *ILZRO Project LE-276 Rep. No. 7 and 8*, International Lead Zinc Research Organization, Research Triangle Park, NC, USA, 1982.

3 R. F. Nelson and D. M. Wisdom, *J. Power Sources, 33* (1991) 165–185.
4 T. G. Chang, in K. R. Bullock and D. Pavlov (eds.), *Proc. Symp. Advances in Lead-Acid Batteries,* Vol. 84-14, The Electrochemical Society, Pennington, NJ, USA, 1984, pp. 86–97.
5 H. Nakashima and S. Hattori, *Proc. Pb80 Int. Lead Conf., Madrid, Spain, 1980,* p. 80.
6 U. Hullmeine, E. Voss and A. Winsel, *J. Power Sources, 30* (1990) 99–105.
7 D. Pavlov and E. Bashtavelova, *J. Electrochem. Soc., 131* (1984) 1468–1476; *133* (1986) 241–248.
8 D. Pavlov, I. Balkanov and P. Rachev, *J. Electrochem. Soc., 134* (1987) 2390–2398.
9 J. S. Newman and C. W. Tobias, *J. Electrochem. Soc., 109* (1962) 1183–1191.
10 K. Micka and I. Rousar, *Electochim. Acta, 18* (1973) 629; *21* (1979) 921–930.
11 J. Burbank, *J. Electrochem. Soc., 111* (1964) 765–770; *111* (1964) 1112–1118.
12 E. J. Ritchie and J. Burbank, *J. Electrochem. Soc., 116* (1969) 125–133; *117* (1970) 299–305.
13 D. Pavlov, E. Bashtavelova and V. Iliev, in K. R. Bullock and D. Pavlov (eds.), *Proc. Symp. Advances in Lead-Acid Batteries,* Vol. 84-14, The Electrochemical Society, Pennington, NJ, USA, 1984, pp. 16–32.
14 A. Winsel, E. Voss and U. Hullmeine, *J. Power Sources, 30* (1990) 209–226.
15 S. M. Caulder, J. S. Murday and A. C. Simon, *J. Electrochem. Soc., 120* (1973) 1515–1522.
16 S. M. Caulder and A. C. Simon, *J. Electrochem. Soc., 121* (1974) 1546–1551.
17 S. M. Caulder, A. C. Simon and J. T. Stemmle, *J. Electrochem. Soc., 122* (1975) 461–466; *122* (1975) 1640–1648.
18 A. C. Simon and S. M. Caulder, in D. H. Collins (ed.), *Power Sources 5, Research and Development in Non-Mechanical Electrical Power Sources,* Academic Press, London, 1975, pp. 109–121.
19 J. P. Pohl and H. Rickert, in D. H. Collins (ed.), *Power Sources 5, Research and Development in Non-Mechanical Electrical Power Sources,* Academic Press, London, 1975, pp. 15–21.
20 G. P. Papazov, J. P. Pohl and H. Rickert, in J. Thompson (ed.), *Power Sources 7, Research and Development in Non-Mechanical Electrical Power Sources,* 1979, pp. 37–43.
21 J. P. Pohl, *Prog. Battery Solar Cells, 5* (1984) 174–182.
22 J. P. Pohl and G. L. Schlechtriemen, *J. Appl. Electrochem., 14* (1984) 521–531.
23 J. D. Jorgensen, R. Varma, F. J. Rotella, G. Cook and N. P. Yao, *J. Electrochem. Soc., 129* (1982) 1678–1681.
24 R. J. Hill and I. C. Madsen, *J. Electrochem. Soc., 131* (1984) 1486–1491.
25 R. J. Hill, A. M. Jessel and I. C. Madsen, in K. R. Bullock and D. Pavlov (eds.), *Proc. Symp. Advances in Lead-Acid Batteries,* Vol. 84-14, The Electrochemical Society, Pennington, NJ, USA, 1984, pp. 59-77.
26 R. J. Hill and M. R. Houchin, *Electrochim. Acta, 30* (1985) 559–573.
27 R. J. Hill, D. A. J. Rand and R. Woods, in L. J. Pearce (ed.), *Power Sources 11, Research and Development in Non-Mechanical Electrical Power Sources,* Int. Power Sources Symp. Committee, Leatherhead, UK, 1987, p. 103.
28 N. J. Maskalick, *J. Electrochem. Soc., 122* (1975) 19–30.
29 V. H. Dodson, *J. Electrochem. Soc., 108* (1961) 406–412.
30 F. Caldera, A. Dalmastro, G. Fracchia and M. Maja, *J. Electrochem. Soc., 127* (1980) 1869–1879.
31 S. Tudor, A. Weisstuch and S. H. Dowang, *Electrochem. Technol., 3* (1965) 90–94; *4* (1966) 406–411; *5* (1967) 21–26.
32 J. L. Weininger and E. G. Siwek, *J. Electrochem. Soc., 123* (1976) 602–606.
33 D. Barrett, M. T. Frost, J. A. Hamilton, K. Harris, I. R. Harrowfield, J. F. Moresby and D. A. J. Rand, *J. Electrounal. Chem., 118* (1981) 131–155.
34 S. Hattori, M. Yamashita, M. Kono, M. Yamane, M. Nakashima and J. Yamashita, *ILZRO Projects LE-253 and LE-276,* Ann. Rep. 1978 and 1979, International Lead Zinc Research Organization, Research Triangle Park, NC, USA.
35 D. Pavlov and N. Iordanov, *J. Electrochem. Soc., 117* (1970) 1103–1109.
36 D. Pavlov and R. Popova, *Electrochim. Acta, 15* (1970) 1483–1491.
37 P. Ruetschi, *J. Electrochem. Soc., 120* (1973) 331–337.
38 J. Garche, *J. Power Sources, 30* (1990) 47–54.

39 H. K. Giess, in K. R. Bullock and D. Pavlov (eds.), *Proc. Symp. Advances in Lead-Acid Batteries,* Vol. 84-14, The Electrochemical Society, Pennington, NJ, USA, 1984, pp. 241–251.
40 D. Pavlov, B. Monachov, M. Maja and N. Penazzi, *J. Electrochem. Soc., 136* (1989) 27–33.
41 H. Doring, J. Garche, H. Dietz and K. Wiesener, *J. Power Sources, 30* (1990) 41–46.
42 D. L. Douglas and G. W. Mao, in D. H. Collins (ed.), *Power Sources 4, Research and Development in Non-Mechanical Electrical Power Sources,* Oriel Press, Newcastle upon Tyne, 1973, pp. 561–567.
43 B. K. Mahato, *J. Electrochem. Soc., 126* (1979) 365–370.
44 D. C. Constable, J. K. Gardner, J. A. Hamilton, K. Harris, R. J. Hill, D. A. J. Rand, S. Swan and L. B. Zalcman, *ILZRO Project LE-290,* Annu. Rep. 1982; *J. Power Sources, 23* (1988) 257–277.
45 S. Hattori, M. Yamaura, M. Kono, M. Yamane, H. Nakashima, J. Yamashita and J. Nakayama, *ILZRO Project LE-276,* Rep. No. 5, 1980.
46 D. Pavlov, E. Bashtavelova, V. Manevand and A. Nasalevska, *J. Power Sources, 19* (1987) 15.
47 D. Pavlov, I. Balkanov, T. Halachev and P. Rachev, *J. Electrochem. Soc., 136* (1989) 3189–3197.
48 D. Pavlov and I. Balkanov, *J. Electrochem. Soc., 139* (1992) 1830–1835.
49 D. Pavlov, *J. Electrochem. Soc., 139* (1992) 3075–3080.
50 D. Pavlov, A. Dakhouche and T. Rogachev, *J. Power Sources, 42* (1993) 71–87.
51 E. M. L. Valeriote, A. Heim and M. A. Ho, *J. Power Sources, 33* (1991) 187–212.
52 D. Pavlov, A. Dakhouche and T. Rogachev, *J. Power Sources, 30* (1990) 117–130.
53 B. Monahov and D. Pavlov, *J. Appl. Electrochem.,* in press.
54 D. Pavlov, B. Monahov, G. Sundholm and T. Laitinen, *J. Electroanal. Chem., 305* (1991) 57–72.
55 J. L. Dawson, M. I. Gillibrand and J. Wilkinson, in D. H. Collins (ed.), *Power Sources 3, Research and Development in Non-Mechanical Electrical Power Sources,* Oriel Press, Newcastle upon Tyne, 1970, pp. 1–9.
56 J. L. Dawson, J. Wilkinson and M. I. Gillibrand, *J. Inorg. Nucl. Chem., 32* (1970) 501–517.
57 J. J. Lander, *J. Electrochem. Soc., 98* (1951) 213–219; *98* (1951) 220–226; *102* (1956) 1–8.
58 K. R. Bullock and M. A. Butler, *J. Electrochem. Soc., 133* (1986) 1085–1091.
59 D. Pavlov and St. Ruevski, *J. Electrochem. Soc., 126* (1979) 1100–1104.
60 J. Garche, N. Anastasijevic and K. Wiesener, *Electrochim. Acta, 26* (1981) 1363–1375.
61 K. R. Bullock and E. C. Laird, *J. Electrochem. Soc., 129* (1982) 1393–1399.
62 K. Takahashi, H. Yasuda, N. Takami, S. Horie and Y. Suzui, *J. Power Sources, 36* (1991) 451–460.